J. Physiol. (1980), **301**, *pp.* 157–173
With 10 *text-figures*
Printed in Great Britain

MEMBRANE ELECTRICAL PROPERTIES OF FROG SLOW MUSCLE FIBRES

BY W. F. GILLY* AND CHIU SHUEN HUI†
From the Department of Physiology, Yale University Medical School, 333 Cedar Street, New Haven, Connecticut 06510, U.S.A.

(*Received 26 April 1979*)

SUMMARY

1. Pyriformis slow (and sartorius twitch) fibres from *Rana temporaria* were studied with a three-micro-electrode voltage-clamp technique to obtain an approximate measurement of membrane current density at a fibre end. In most experiments, a modified Ringer solution containing ^2H_2O and 230 mM-sucrose was used to reduce movement.

2. Linear membrane properties of slow fibres obtained with this method are consistent with results from previous studies. Measured C_m (μF/cm^2) increases with fibre diameter in a manner consistent with a tubular location of part of the fibre capacitance.

3. Voltage steps to -50 mV and more positive potentials result in outward membrane currents in both slow and twitch fibres. These currents develop along similar sigmoid time courses and are blocked by tetraethylammonium (TEA^+) ions. The reversal potential for delayed current channels in slow fibres varies with external K^+ concentration, suggesting that the delayed current in slow fibres, as in twitch, is carried by K^+ ions.

4. Maximum G_K, $\bar{G}_K$, in slow fibres is an order of magnitude smaller than in twitch fibres. The steady-state G_K–V curve of slow fibres is very broad (e-fold for $\sim$ 15 mV), saturating at very positive voltages, whereas the G_K of twitch fibres varies more steeply with voltage.

5. No evidence of inward currents was seen in slow fibres during pulses of duration up to 96 msec.

6. Slow outward currents, which do not inactivate appreciably, are seen in slow fibres during long (10 sec) pulses. Tail currents following such long pulses are very slow. The reversal potential shifts to more positive values with increasing pulse duration.

INTRODUCTION

Membrane electrical properties of frog slow muscle fibres have been studied in the past with micro-electrode methods. A basic difficulty with these techniques is that the specific membrane resistance in these fibres is so high that insertion of a micro-

* Present address: Biology Department/G5, University of Pennsylvania, Philadelphia, Pennsylvania 19104, U.S.A.

† To whom reprint request should be sent. Present address: Department of Biological Sciences, Purdue University, West Lafayette, Indiana 47907, U.S.A.

0022-3751/80/7170-0168 $07.50 © 1980 The Physiological Society

electrode results in a leak conductance large enough to shunt the resting potential appreciably (Stefani & Steinbach, 1969). The resting membrane of a slow fibre is a fairly good K^+ electrode. Permeability to Cl^- must be extremely low as total replacement of external Cl^- by methyl sulphate does not cause a depolarization large enough to activate contraction (Nasledov, Zachar & Zacharova, 1966).

Ordinarily, slow fibres are not able to generate action potentials (Kuffler & Vaughan Williams, 1953) and, presumably, lack voltage-dependent Na^+ channels. Voltage-dependent Ca^{2+} channels are probably present in the slow fibre membrane, but not in sufficient number to enable any sort of regenerative response in low K^+ solutions (Stefani & Uchitel, 1976). A voltage- and time-dependent K^+ permeation system is though to be present in slow fibres, based on the observation of a substantial repolarization following activation by synaptic potentials or electrotonic responses to depolarizing current pulses (Burke & Ginsborg, 1956). Owing to limitations of the methods used in these studies, properties of the ion permeation systems in slow fibres have not been well characterized.

The voltage-clamp studies described in this report were carried out to obtain additional information about the electrical properties of slow fibres. The three-micro-electrode voltage-clamp technique developed by Adrian, Chandler & Hodgkin (1970*a*) was used to measure membrane current density and to characterize the ion permeation systems. Preliminary reports of this work have appeared (Hui & Gilly, 1977; Chandler, Gilly & Hui, 1978).

METHODS

Experiments were carried out in the same manner as those described in the preceding paper (Gilly & Hui, 1980*a*), except that fibre type identification was based solely on microscopic appearance and electrical characteristics, since in most experiments contraction was abolished by a 2 times hypertonic ^2H_2O solution. Slow fibres were all from warm-adapted frogs; twitch fibres were from cold-adapted animals.

Twitch fibre diameter was calculated in the usual manner from measured values of input resistance (R_{in}) and space constant (λ) and assumed values of internal resistivity (R_i). Hodgkin & Nakajima (1972) have obtained values of R_i for twitch fibres in normal and 2·5 times hypertonic Ringer solutions at 2 °C. Linear interpolation between these values gives 365·4 Ω.cm for 2 times hypertonic solutions. Q_{10} was assumed to be 1·37 (Hodgkin & Nakajima, 1972). Also, a factor of 1·2 was introduced to account for replacement of H_2O by ^2H_2O (Garby & Nordquist, 1955; Thomson, 1963). Furthermore, R_i depends on sarcomere length (Dulhunty & Franzini-Armstrong, 1977). This might cause an over-estimate of current density in slow fibres by as much as 30% ($\sim$ 3·0 μm sarcomere length) but no correction was made.

Measurements of R_{in} and λ in slow fibres using micro-electrodes are extremely dependent on the leakage conductance at impalement sites and realistic values for fibre diameter cannot be thus obtained. Diameters were, therefore, measured optically in normal Ringer solution and multiplied by $\sqrt{0{\cdot}68} = 0{\cdot}82$ to convert to values in 2 times hypertonic solutions (Blinks, 1965). This shrinkage factor was measured in two cases by comparing diameters measured at several points along the length of a slow fibre (near the femoral end) in the two solutions. In both fibres a value of 0·78 was obtained. R_i in slow fibres was assumed to be the same as that in twitch fibres and to be identically affected by ^2H_2O.

Three-micro-electrode voltage clamp was applied to the end of muscle fibres (Adrian *et al.* 1970*a*). For these experiments, the extracellular and three intracellular electrodes were shielded. Shields for the three voltage electrodes were driven at unity gain by the respective electrometer outputs, and the current electrode shield was grounded. Command pulses to the voltage-clamp circuit were deliberately rounded with time constants of 120 μsec (for clamping V_2) or 360 μsec (for clamping V_1).

According to the theory of three-micro-electrode voltage clamp, the membrane current density is proportional to ΔV, the difference between V_1 and V_2 measured by the two intracellular voltage electrodes. Both ΔV and the controlled membrane potential signals were filtered (at 1 kHz) and amplified by instrumentation amplifiers, sampled by an ADAC A/D converter, and stored in a PDP 11/03 computer. Sampling rate was adjusted to match the time course of the process under investigation.

TABLE 1. Composition of solutions (mM)

Solution	NaCl	KCl	Tetraethyl-ammonium Cl	$CaCl_2$	Sucrose
A, (normal Ringer) (H_2O)	115	2·5	—	1·8	—
B (H_2O)	115	2·5	—	11·8	—
C (^2H_2O)	120	2·5	—	1·8	230
D (^2H_2O)	120	2·5	—	11·8	230
E (^2H_2O)	—	2·5	115	11·8	230

All solutions were buffered to pH 7·0 or pD 7·4 (Nakajima & Kuroda, 1976): solutions A and C with 1·1 mM-Na_2HPO_4 and 0·4 mM-NaH_2PO_4; solutions B, D and E with 1·0 mM-PIPES buffer (1,4-piperazinediethane sulphonic acid).

Correction of membrane current traces for linear capacitive and ionic leakage components was achieved by appropriate scaling and subtraction of control currents from test currents. A control pulse (usually 20 mV) was superimposed on a hyperpolarizing pre-pulse of equal magnitude. Test and control traces were signal-averaged whenever necessary.

Solutions used are given in Table 1. Tetrodotoxin was added to all Ringer solutions for twitch fibre experiments (10 μg/ml.), but was omitted for all slow fibre experiments.

RESULTS

Resting membrane conductance of slow fibres

Fig. 1 shows photographic records obtained with the three-electrode voltage clamp. Steps of $\pm$ 5·6 mV were imposed at V_2 on a slow fibre in normal Ringer solution, and V_1 (upper), V_2 (middle), and I_0 (lower) traces are shown in Fig. 1*A*. Fig. 1*B* shows ΔV (upper trace) and V_2 (lower trace) for brief pulses at a high sweep speed. Following the step in V_2, ΔV shows a capacitive transient which decays, with a time constant of 1·25–1·5 msec, to a steady-state level proportional to membrane ionic current and any leakage conductance at the V_1 impalement site (Appendix A in Schneider & Chandler, 1976). The steady-state level is probably less than half the base line width, 0·1 mV, which corresponds to a lower limit of $1{\cdot}5 \times 10^4\ \Omega.\mathrm{cm}^2$ for R_m. This value is substantially lower than the $1{\cdot}1 \times 10^5\ \Omega.\mathrm{cm}^2$ value for slow fibres obtained by Stefani & Steinbach (1969), using a much larger electrode spacing. The diminution may be largely due to leakage current at the V_1 impalement site.

The relative contribution of the leakage resistance (R_L) can be estimated from:

$$I_m = \frac{d}{6R_i l^2}\Delta V - \frac{2}{3\pi d l R_L}V_1 \qquad (1)$$

(Schneider & Chandler, 1976, Appendix A). With the assumed ΔV of 0·1 mV, V_1 of 5·5 mV, and a true R_m of $10^5\ \Omega.\mathrm{cm}^2$, R_L would be 23·6 MΩ. This could be the actual value since R_{in} measured with two electrodes (V_1 and I) in the fibre was 12·5 MΩ. Conversely, with R_L = 25 MΩ, R_m

would be $7{\cdot}9 \times 10^4\ \Omega.\text{cm}^2$, in fair agreement with Stefani & Steinbach's value. From the voltage decrement measured with two voltage electrodes 1 mm apart, R_m would probably be $> 1{\cdot}5 \times 10^5\ \Omega.\text{cm}^2$ (authors' unpublished results).

Frog slow fibres have also been reported to show a linear relation between membrane potential and I_0 for hyperpolarizing current pulses, i.e. the resting K^+ perme-

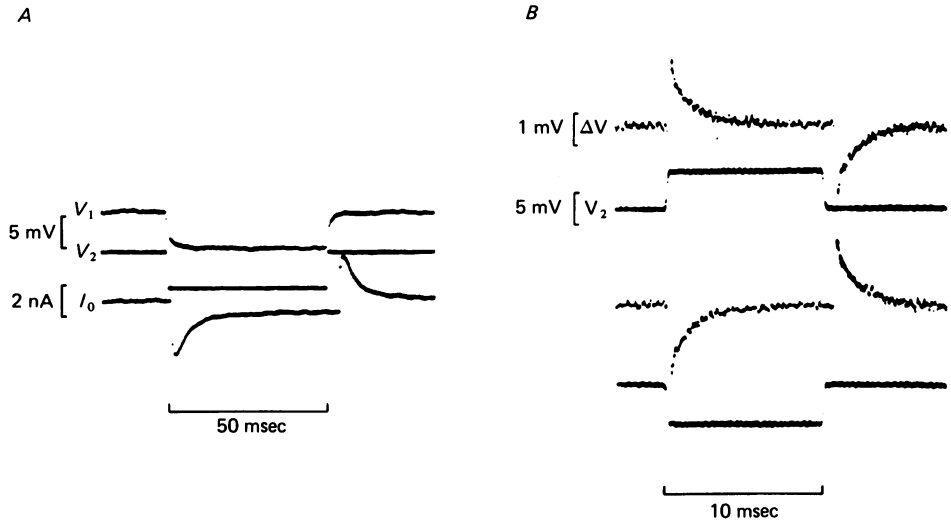

Fig. 1. Current transients in response to small membrane potential changes in a slow fibre. Feed-back control was taken from V_2. Holding potential = −90 mV. Fibre 0702-76. Normal Ringer (solution A); 8·7 °C; l_1 = 417 μm; l_2 = 275 μm; l' = 71 μm; d = 56 μm; R_i assumed to be 249 Ω.cm; total holding current (I_H) = −2 nA; input resistance (R_{in}) = $12{\cdot}5 \times 10^6\ \Omega$ (two electrodes). *A*, membrane potentials V_1 and V_2 along with total current I_0. *B*, depolarizing and hyperpolarizing steps in V_2 with corresponding membrane currents, ΔV ($= V_2 - V_1$). 1 mV in ΔV corresponds to 3·7 μA/cm².

ability does not show inward rectification (Stefani & Steinbach, 1969). Fig. 2 shows I–V plots for a fibre in normal Ringer solution (*A*) and another fibre in a hypertonic ^2H_2O solution (*C*). Both plots are very linear, but again electrode shunt current may have masked some inward rectification. If R_m is actually $10^5\ \Omega.\text{cm}^2$, an increase in membrane slope conductance at highly negative potentials by a factor as small as 2–3 should have been detectable. Thus, within the resolution of the method, the slow fibre membrane does not show inward rectification to the extent that frog twitch fibres do (Adrian, 1964).

Linear membrane capacitance of slow fibres

Although direct measurement of R_m from ΔV traces may not be very reliable in slow fibres, a good estimate of $r_i\ c_{eff}$ (r_i = internal resistivity per unit length and c_{eff} = the effective fibre capacitance per unit length) can be obtained by integration of the transient current as described by Schneider & Chandler (1976). To obtain C_{eff} (in μF/cm²) from this product, values of R_i and fibre diameter are required. The

former is assumed from known values in twitch fibres, as mentioned in the Methods, and the latter was measured optically, which may introduce some error.

Traces shown in Fig. 1*B* give a value of about 1·7 μF/cm^2 for C_m (referred to cylindrical fibre area) for a fibre of diameter 56 μm. A total of six fibres, diameters

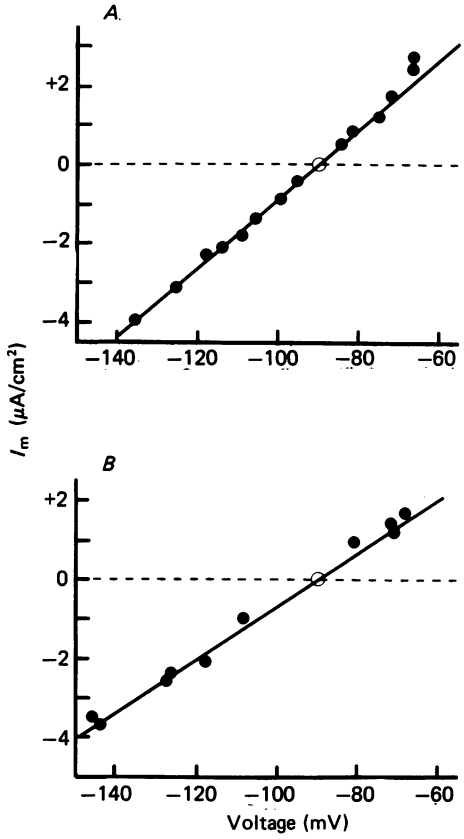

Fig. 2. Steady-state *I–V* relations for slow fibres below the threshold for delayed rectification. 0: indicates holding potential; holding current taken as zero reference. *A*, fibre 0141-76 in normal Ringer (solution A); 8·4 °C; $l_1 = l_2 = 393$ μm; $l' = 134$ μm; $d = 44$ μm; sarcomere length = 2·80 μm; control taken from V_2; $R_i = 244$ Ω.cm; $C_m = 2{\cdot}9$ μF/cm^2; 1 mV in $\Delta V = 2{\cdot}07$ μA/cm^2; $I_H = -50$ nA; $R_{in} = 6 \times 10^6$ Ω (three electrodes). $R_m = 1{\cdot}1 \times 10^4$ Ω.cm^2, not corrected for electrode leak. *B*, fibre 0192-76 in ^2H_2O Ringer solution containing 230 mM-sucrose (solution C); 5·6 °C; $l_1 = l_2 = 393$ μm; $l' = 65$ μm; d = 50 μm; sarcomere length = 3·22 μm; control taken from V_2; $R_i = 392$ Ω.cm; $C_m = 3{\cdot}4$ μF/cm^2; 1 mV in $\Delta V = 1{\cdot}38$ μA/cm^2; $I_H = -20$ nA; $R_{in} = 3 \times 10^6$ Ω (three electrodes). $R_m = 1{\cdot}6 \times 10^4$ Ω.cm^2, not corrected.

40–60 μm, gave a mean value of 4·0 μF/cm^2 (range 1·7–6·9) for C_m in isotonic solutions. C. H. Bailey & L. D. Peachey (in preparation) give a tubular:surface area ratio of 2·5 for a 50 μm diameter slow fibre. Thus, the apparent C_m should be about 3·5 μF/cm^2, assuming a specific surface and tubular capacitance of 1 μF/cm^2. Surface membrane infoldings and caveolae probably exist in slow fibres (personal communication from C. Franzini-Armstrong), as in twitch fibres, and the fibre surface area

might be increased by a factor as large as 1·9 (Dulhunty & Franzini-Armstrong, 1975), bringing the expected C_m up to 4·4 μF/cm^2. Our results agree fairly well with this.

A plot of C_m *vs.* diameter is shown in Fig. 3 for slow fibres studied in isotonic Ringer solutions. Although the scatter in the data is large, probably due to the errors discussed above, there is a tendency for C_m to increase with diameter. The

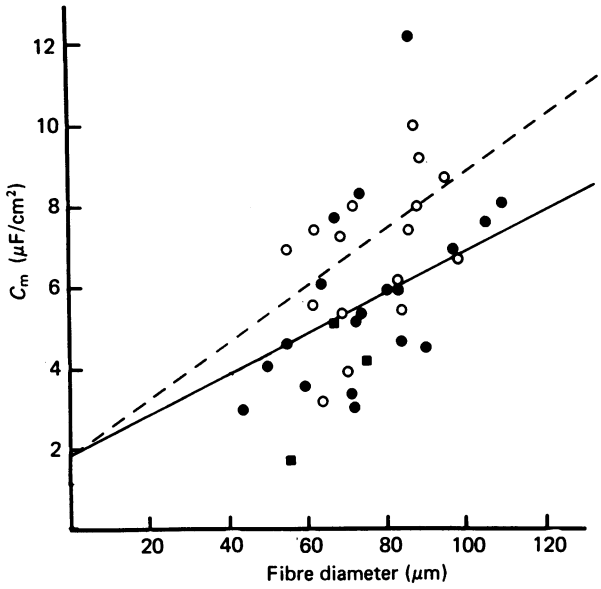

Fig. 3. Dependence of membrane capacitance on fibre diameter in slow fibres studied in isotonic solutions. ■, normal Ringer (solution A); ●, normal Ringer solution with 2 mM-tetracaine; ○, high Ca^{2+} Ringer (solution B) with 2 mM-tetracaine. Fibre diameters were determined optically (Gilly & Hui, 1980*a*). The continuous line has been drawn for slow fibres according to the equation: $C_m = 1{\cdot}9 + 0{\cdot}05\,d$ (see text), and the dashed line for twitch fibres according to the equation: $C_m = 1{\cdot}9 + 0{\cdot}07\,d$ (Peachey, 1965). Holding potential was -80 to -100 mV; control point at V_2; 5–10 °C.

continuous line has been drawn through the points 1·9 μF/cm^2 (at 0 μm) and 4·4 μF/cm^2 (at 50 μm); the dashed line is the corresponding relation for twitch fibres (Hodgkin & Nakajima, 1972).

In general, values of membrane capacitance obtained with the present method are in fair agreement with those from constant current pulse measurements (Adrian & Peachey, 1965; Stefani & Steinbach, 1969).

Membrane currents upon depolarization

In order to measure membrane currents at potentials more positive than contraction threshold, it is necessary to block fibre contraction. Strongly hypertonic solutions proved unsuitable because they caused slow fibres to go into strong maintained contracture. ^2H_2O is known to diminish the twitch of frog muscle (Svensmark, 1961; Godt, Allen & Blinks, 1978). A ^2H_2O Ringer solution containing 230 mM-sucrose (approximately 2 times hypertonic) appeared to be more suitable as contractions were virtually abolished even with very strong and long depolarizations. Such ^2H_2O

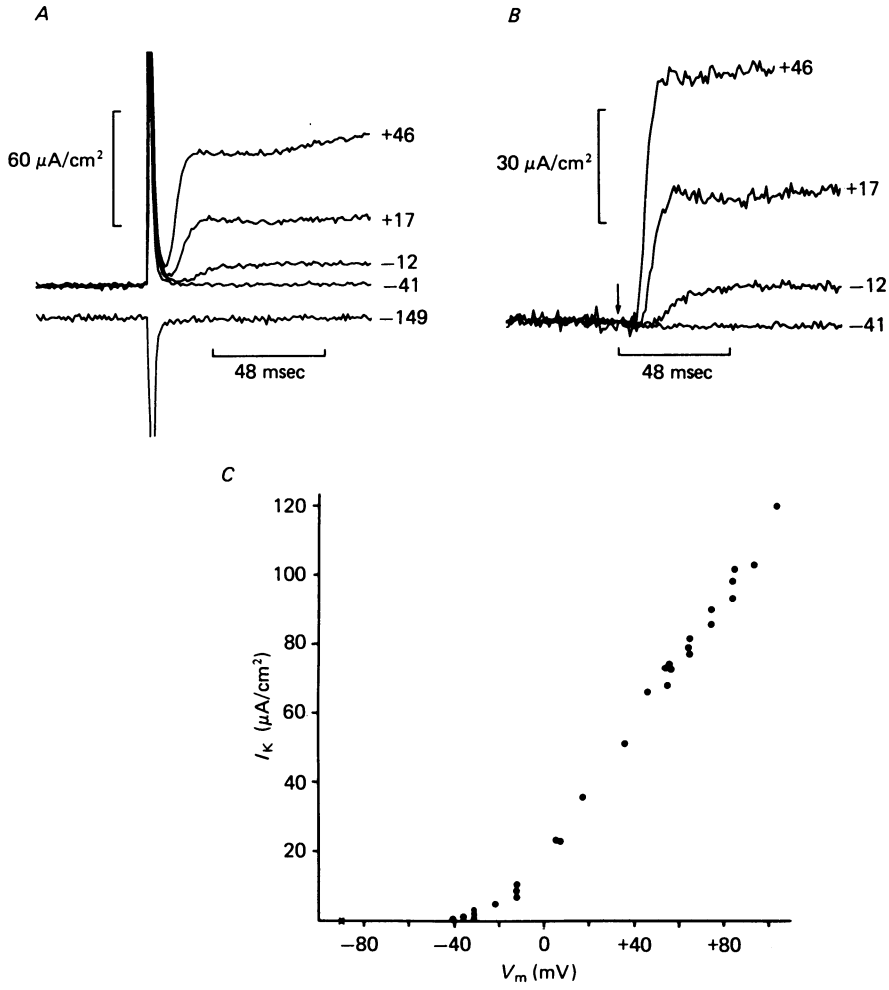

Fig. 4. Membrane ionic currents in slow fibres during depolarizations in hypertonic ^2H_2O Ringer solution. *A*, ΔV traces showing the initial surge of capacitive current and both linear and non-linear, time-dependent components of ionic current. Control taken from V_1. Fibre 9173-77, solution D; 9·9 °C; holding potential = −90 mV; $l_1 = l_2 = 156\ \mu m$; $l' = 40\ \mu m$; sarcomere length = 2·90 μm; $C_m = 6{\cdot}5\ \mu F/cm^2$; $R_i = 341\ \Omega.cm$; 1 mV in $\Delta V = 11{\cdot}0\ \mu A/cm^2$. *B*, traces of outward membrane ionic current from the records in *A* after correction for linear capacitive and ionic leakage currents (as described in text). Traces have been terminated at the estimated onset of the slow component of current. *C*, membrane current–voltage relation from final currents in *B*.

solutions were, therefore, used for both slow and twitch fibre experiments, although they did not seem to be as effective in blocking movement in the latter.

Membrane currents from a slow fibre held at −90 mV are shown in Fig. 4. Fig. 4*A* shows records from a fibre clamped at V_1. For a small depolarization or hyperpolarization, there is a surge of capacitive current, followed by an ionic current which reaches a steady amplitude during the pulse. For stronger depolarizations, a second slower component of outward current often developed. Both fast and slow components were

variable in their amplitudes from fibre to fibre, similar to observations on twitch fibres (Lynch 1978*a*, *b*).

In order to study the fast component of outward current better, it is useful to remove the linear capacitive and leakage ionic components of membrane current. Results are shown in Fig. 4*B*. As in twitch fibres, outward currents develop along a

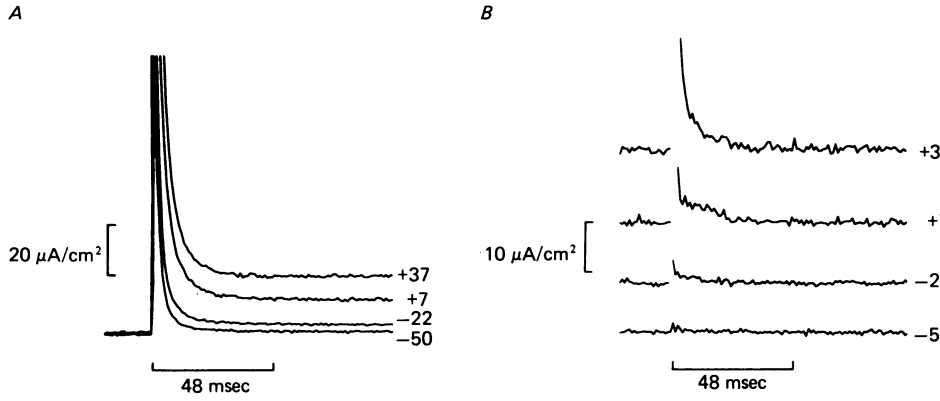

Fig. 5. Effect of TEA^+ on delayed K^+ currents. *A*, current traces for depolarizations to voltages as indicated in mV at the right. Fibre 9221-77. $d = 49{\cdot}1\ \mu m$; $l = 234\ \mu m$; $l' = 40\ \mu m$; $R_i = 274{\cdot}6\ \Omega.cm$; holding potential $= -80$ mV; sarcomere length $= 3{\cdot}25\ \mu m$; solution E; 9·9 °C; control taken from V_1; 1 mV in $\Delta V = 3{\cdot}99\ \mu A/cm^2$. *B*, current traces from *A* after subtraction of linear capacitive and leakage ionic currents. The following erratic points have been omitted at the make of the depolarizing pulse: first three points (top trace), first two points (second trace), and first point (third trace).

sigmoidal time course, and the rate of current development increases substantially as the membrane potential becomes more positive. Fig. 4*C* shows the steady-state current–voltage relation for the fast component of outward membrane current in 4*B*. Membrane slope conductance increases sharply around -40 mV. Net inward currents were never observed in slow fibres.

Similar experiments were carried out in the presence of TEA^+ ions. Isotonic TEA^+ blocks about 90% of the fast delayed rectifier K^+ conductance in frog twitch fibres (Stanfield, 1970), and TEA^+ ions block similar K^+ currents in a variety of excitable membranes. Records obtained from a fibre in high Ca^{2+}, TEA^+ Ringer (solution E) are shown in Fig. 5*A*. Fig. 5*B* shows the same records after removal of linear capacitive and ionic currents from the traces. There is no sign of delayed outward currents nor of inward currents. Only voltage dependent non-linear capacitive currents (charge movements) remain at the make and the break (not shown) of the pulses. Properties of such capacitive currents will be described in the following paper (Gilly & Hui, 1980*b*).

The time course of the outward currents in slow fibres and the effect of TEA^+ suggest that they might be carried by K^+ ions and that they might be analogous to the delayed K^+ currents in twitch fibres.

Reversal potential of the fast K+ currents

Depolarizing pulses (24 msec duration and 100 mV amplitude) were applied to slow fibres to activate a substantial amount of the K^+ conductance, and tail currents were obtained by taking the membrane potential to various levels immediately following the pulses. In an experiment in 2·5 mM-K^+ Ringer solution, the tail currents

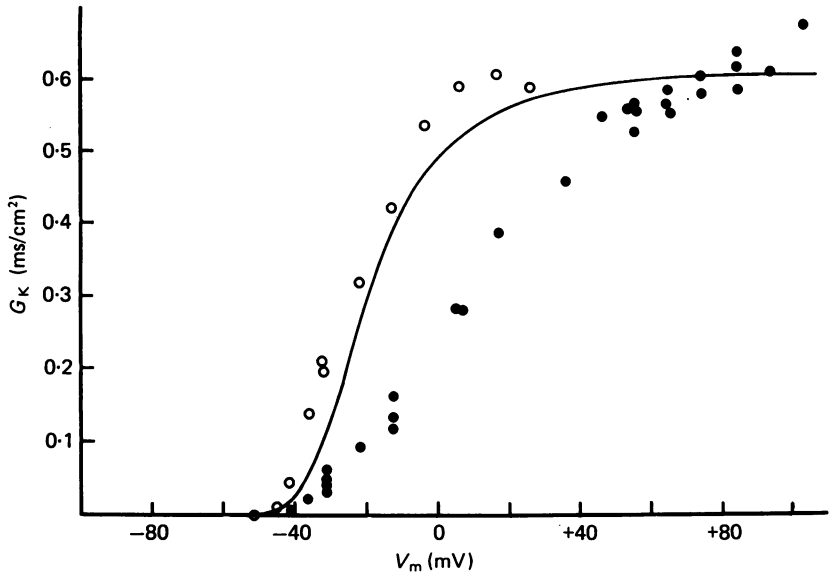

Fig. 6. Comparison of G_K–V relation between slow and twitch fibres. ●, steady-state G_K–V relation for the slow fibre in Fig. 4. Fibre movement was not visually detected in this fibre at any voltage with 96 msec pulses. ○, G_K–V relation for a twitch fibre in solution D. Control was taken from V_1. Fibre 8122-77. 9·6 °C; holding potential = −90 mV; l = 156 μm; l' = 40 μm; R_{in} = 700 × 10^3 Ω; λ = 0·84 mm; R_i = 341 Ω.cm; d = 65 μm; C_m = 20 μF/cm². V_K was assumed to be −85 mV (Adrian *et al.* 1970*a*). G_K values have been scaled down by a factor of 0·046. The continuous curve was drawn for the n^4 (∞) relation for twitch fibres according to Adrian *et al.* (1970*a*), but scaled to match the slow fibre $\bar{G}_K$ and shifted 7 mV to the right to allow for the 11·8 mM-Ca^{2+} (Costantin, 1968).

clearly changed sign, from inward at −101 mV to outward at −51 mV. The true value of reversal potential is difficult to determine, primarily because of the small magnitude of the tail currents and a substantial contamination by charge movement (Gilly & Hui, 1980*b*). Taking this contamination into account, the reversal potential in 2·5 mM-K^+ probably lies between −80 and −70 mV, and a value of −75 mV will be assumed in the following analysis.

Similar experiments in solutions with elevated K^+ yielded more positive values of reversal potential. Two experiments in 16 mM-K^+ gave values between −40 and −50 mV, while a fibre studied in 28 mM-K^+ gave a value near −30 mV. All these values are approximate, but they do suggest that the channel mediating the fast delayed outward current is primarily a K^+ channel.

Voltage dependence of the fast K^+ conductance

In a frog twitch fibre the delayed K^+ channels show a linear instantaneous $I-V$ relation, and the conductance can be written as

$$G_K = \frac{I_K}{V - V_K}, \tag{2}$$

where V_K is the observed reversal potential (Adrian *et al.* 1970*a*). This equation was used to obtain values of G_K (of fast component) from Fig. 4*C*, and the closed circles of Fig. 6 show the G_K–V relation. For this fibre, the saturating value of G_K, $\bar{G}_K$, is 0·6 mS/cm². Values from four other slow fibres averaged 0·7 mS/cm² (range 0·5–0·9 mS/cm²), and three additional fibres studied in a 16 mM-K^+ Ringer solution gave a mean $\bar{G}_K$ of 0·5 mS/cm² (range 0·3–0·8 mS/cm²). These values are an order of magnitude smaller than those observed in twitch fibres, 2–10 mS/cm² (isotonic H_2O, Almers, 1976), 8·5–20 mS/cm² (hypertonic H_2O, Adrian *et al.* 1970*a*) and 6–20 mS/cm² (solution D, authors' unpublished results). The difference is equally large if the analysis is carried out using permeability rather than conductance.

Fig. 6 shows another important difference between the steady-state G_K–V relations in slow and twitch fibres. The continuous curve is drawn according to the equation for n^4 (V) given by Adrian *et al.* (1970*a*) for twitch fibres and scaled to match the slow fibre $\bar{G}_K$. The curve does not fit the slow fibre data. The discrepancy is not due to replacement of H_2O by ^2H_2O, as evidenced by the open circles obtained from a twitch fibre in the same hypertonic ^2H_2O solution.

Kinetics of delayed rectification in slow fibres

Delayed rectification in frog twitch muscle mechanically inactivated by hypertonic H_2O solutions can be described reasonably well by a Hodgkin–Huxley n^4 formulation (Adrian *et al.* 1970*a*; Stanfield, 1970). A semi-log plot of the 'on' or 'off' current *vs.* t should give a straight line, from which τ_n can be measured. Fig. 7*A* shows the delayed K^+ current in a slow fibre during and after a large depolarization. The corresponding semi-log plots are shown in Fig. 7*B*. Straight lines fitted to the points by eye gave 8·8 msec (on) and 10·9 msec (off) for τ_n. These values were used to draw the continuous curves in Fig. 7*A*.

Fits for both 'on' and 'off' are fairly good in this example, but the quality of fit was extremely variable from fibre to fibre. In many fibres, I_K rose after a delay of up to 10–15 msec. This can be seen in the records of Fig. 4. For the depolarization to +17 mV, I_K can be fitted by a τ_n of 3·4 msec after introducing a 11 msec delay. It seems unlikely that such delays could be due to simultaneous activation of an inward current since no inward current was seen when the outward current was blocked by TEA^+. Twitch fibres in the hypertonic ^2H_2O Ringer also showed similar but shorter delays. Almers (1976) has also noted the presence of such a delay in twitch fibres inactivated by tetracaine.

Reciprocals of the 'on' and 'off' τ_n from two slow fibres at 7–10 °C are plotted against membrane potential in Fig. 8. The continuous curve was drawn for twitch fibres at 3 °C according to the equation given by Adrian *et al.* (1970*a*) and agrees fairly well with the filled circles from one fibre. The filled squares from the other fibre have to be multiplied by a factor of 2 (to give the open squares) in order to

obtain a good fit. Taking the temperature difference into consideration, the twitch curve might have to be scaled up by a factor of 2 (Q_{10} = 2·5, Adrian *et al.* 1970*a*). Nonetheless, it can be concluded that the rate constants of fast K^+ conductance changes in slow fibres have similar voltage dependence as, and are at most 2–4

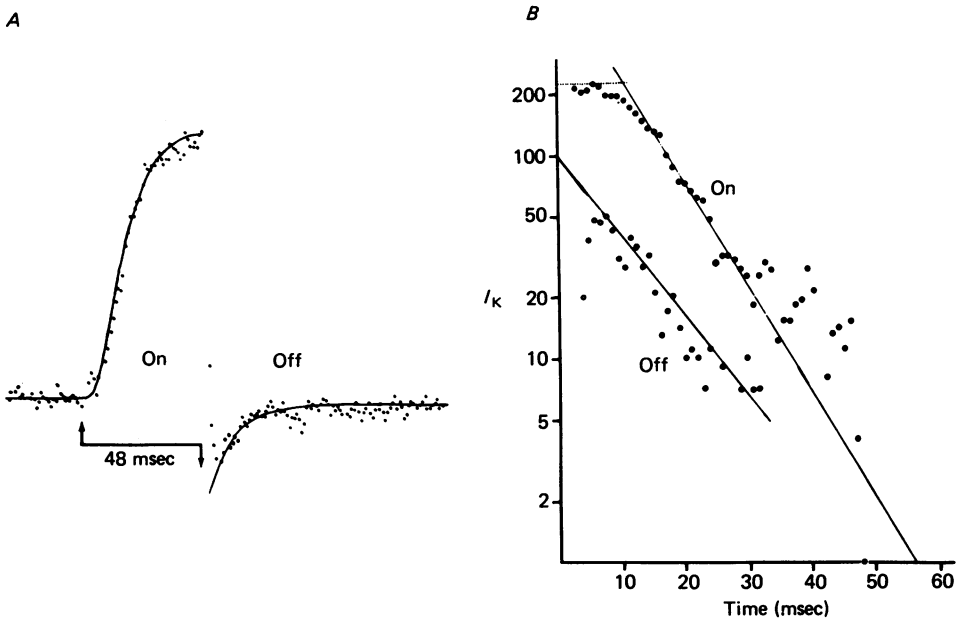

Fig. 7. Analysis of delayed rectifier kinetics. *A*, delayed K^+ current in a slow fibre evoked by a 48 msec pulse to +16 mV from −80 mV after removal of linear components. Arrows indicate make and break of pulse. Control taken from V_1. Fibre 6093·77; solution *D* + 13·5 mM-KCl; 7·1 °C; $l_1 = l_2 = 195\ \mu m$; $l' = 30\ \mu m$; $d = 52{\cdot}7\ \mu m$; $R_i = 375\ \Omega.cm$; 1 mV in $\Delta V = 6{\cdot}1\ \mu A/cm^2$; $I_H = -30$ nA; $R_{in} = 2 \times 10^6\ \Omega$ (three electrodes). Continuous curves are drawn using the τ values from *B*. G_K (∞) is calculated from measured I_K (∞) and $V_K = -50$ mV. *B*, semi-log plots of current during (●) and following (○) the pulse. 'On' current = $I_K(\infty) - I_K(t)$, where $I_K(\infty) = 226$ is the final steady level of I_K at the end of the pulse. 'Off' current = $-I_K(t)$. Base-line of 'on' current was chosen arbitrarily. Several points have been omitted at the make and the break of the pulse. Unit for I_K is arbitrary, 100 ≅ 18 $\mu A/cm^2$.

times smaller than, those in twitch fibres. A small part of this difference may be attributed to the replacement of H_2O by ^2H_2O (see Conti & Palmieri, 1968).

From a theoretical viewpoint, since the G_K–V curves of slow and twitch fibres have different shapes, one would not expect the τ_n–V curves of slow and twitch fibres to be superimposable after scaling. More experiments are required to settle this point.

Outward currents during long depolarizations

Delayed K^+ currents in frog twitch fibres inactivate with a time constant of 0·5–1·0 sec at 20 °C or 1·5–3·0 sec at 3 °C during depolarizations to positive membrane potentials (Adrian *et al.* 1970*a*). We have made similar observations on twitch and slow fibres at 6–10 °C in the hypertonic ^2H_2O Ringer solution. Fig. 9*A* shows records of outward ionic currents during depolarizing pulses of three different durations in a

twitch fibre. The 96 msec pulse (Fig. 9*A*, *a*) shows the fast component of I_K that has been discussed thus far, plus a slower creep in outward current, probably due to activation of the slow K^+ conductance described by Adrian, Chandler & Hodgkin (1970*b*; Lynch, 1978*a*, *b*). Fig. 9*A*, *b* and *c* shows that total outward current reaches

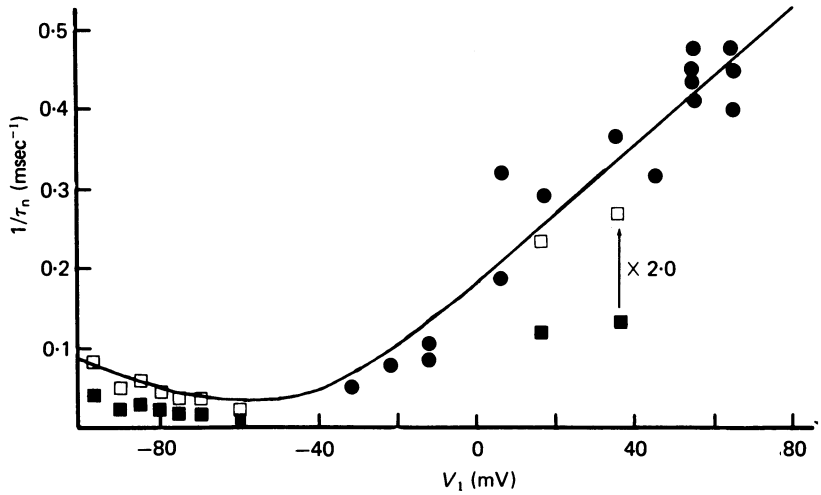

Fig. 8. Comparison of delayed rectifier kinetics in twitch and slow fibres. ■, rate constants from 'on' and 'off' currents from the slow fibre of Fig. 7. These values are also multiplied by 2·0 (represented by □) to facilitate comparison. ●, rate constants from 'on' currents from the slow fibre of Fig. 4. Continuous curve drawn according to Adrian *et al.* (1970*a*) for twitch fibres at 3 °C.

a maximum in about 150 msec and then begins to decline with a time constant of 1–2 sec. Differences in peak current amplitude for the three traces probably reflect fibre deterioration during the course of the experiment, both fast and slow K^+ conductance mechanisms being quite labile.

Fig. 9*B* shows results from an experiment on a slow fibre. Again, fast outward K^+ current develops during the 96 msec pulses (Fig. 9*B*, *a*), and a second slower component of outward current appears during the 960 msec pulses (Fig. 9*B*, *b*). During the 4·8 sec pulses (Fig. 9*B*, *c*) these currents did not inactivate to an appreciable extent. Irregularities on traces for the larger depolarizations are probably due to slight fibre movement. Slow outward currents during 96 msec pulses were nearly completely blocked by TEA^+ (Fig. 5). Except for the lack of inactivation, these results are analogous to those obtained on twitch fibres (Adrian *et al.* 1970*b*; Stanfield, 1970; Lynch, 1978*a*, *b*).

Although separation of the fast and slow current components in slow fibres is difficult, there is no doubt that the slow component in slow fibres has a much smaller magnitude than in twitch.

Slow K^+ current in slow fibres also showed a more positive level of reversal potential and much slower tail current than the fast component. Chart recorder traces of both 0·5 and 10 sec pulses to +5 mV are shown in Fig. 10 and the apparent

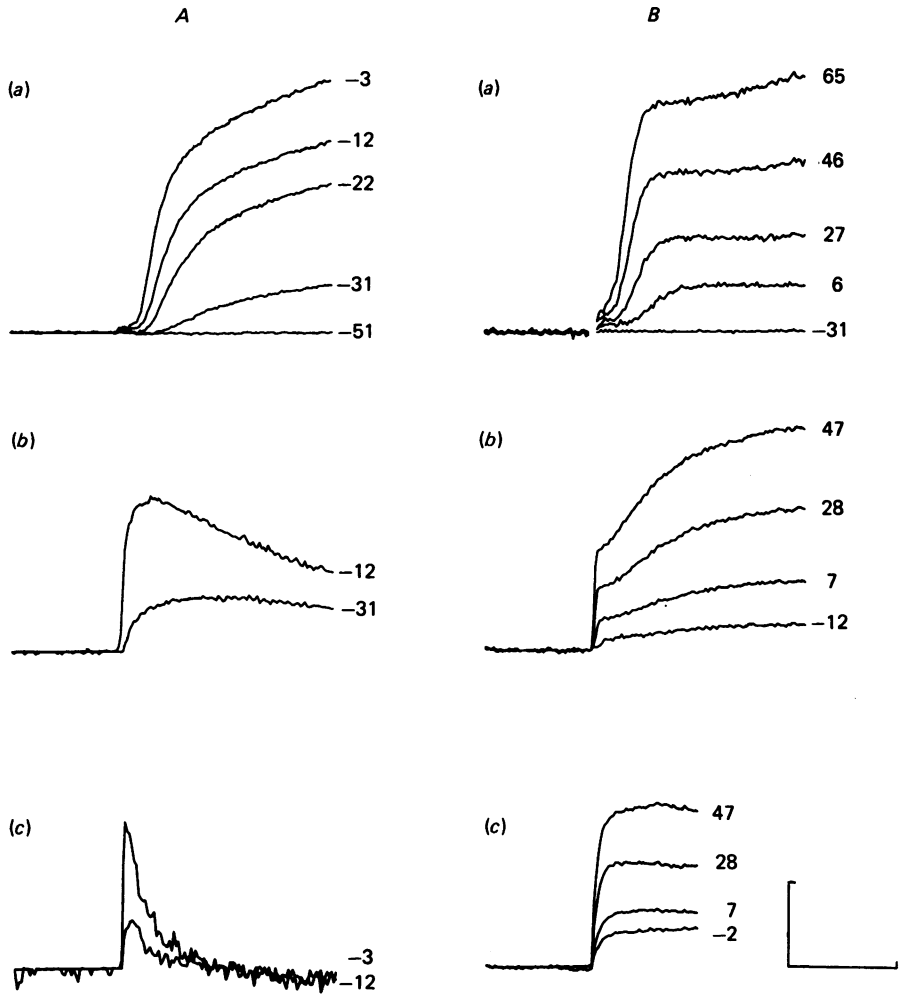

Fig. 9. Delayed outward K^+ currents during pulses of varying duration in twitch and slow fibres. Both fast and slow components of delayed rectification are shown in each fibre type. Vertical scale bar corresponds to 400 μA/cm^2 (*A*,*a*), 200 μA/cm^2 (*A*,*b*), 100 μA/cm^2 (*A*,*c*), and 50 μA/cm^2 (*B*,*a*,*b* and *c*). Horizontal scale bar corresponds to 48 msec (*A*,*a*, *B*,*a*), 480 msec (*A*,*b*, *B*,*b*), and 4·8 sec (*A*,*c*, *B*,*c*). *A*, delayed currents in a twitch fibre during 96 msec (*a*), 960 msec (*b*), and 9·6 sec (*c*) depolarizing pulses to the potentials shown in mV. Control taken from V_1; holding potential = -90 mV. Fibre 8121-77; solution D; 9·7 °C; $l_1 = l_2 = 156$ μm; $l' = 40$ μm; $R_{in} = 580 \times 10^3$ Ω; $\lambda = 1{\cdot}4$ mm (96 msec pulse) and 0·7 mm (for long pulses); R_i assumed to be 341 Ω.cm; $d = 94$ μm (96 msec) and 76 μm (long pulses); $C_m = 25{\cdot}6$ μF/cm^2 initially, decreasing to 13·5 μF/cm^2 at end of experiment. This probably reflects changes in R_i. Fibre deterioration is also suggested by the decreases in λ and peak I_K during the experiment. 1 mV in $\Delta V = 19$ μA/cm^2 (96 msec) or 15 μA/cm^2 (long pulses). Fibre movement occurred with the longest pulse. *B*, delayed currents in a slow fibre during 96 msec (*a*), 960 msec (*b*) and 4·8 sec (*c*) depolarizing pulses to the potentials shown in mV. Control taken from V_1; holding potential = -90 mV. Fibre 9142-77; solution D; 9·8 °C; $l_1 = l_2 = 156$ μm; $l' = 31$ μm; $d = 55{\cdot}0$ μm; sarcomere length = 3·15 μm; R_i assumed to be 341 Ω.cm; $C_m = 11{\cdot}2$ μF/cm^2, decreasing to 8·9 μF/cm^2; 1 mV in $\Delta V = 1$ μA/cm^2; $I_H = -5$ nA; $R_{in} = 17 \times 10^6$ Ω (two and three electrodes). Again, fibre movement probably occurred during some of the longer pulses. Erratic points in *B*,*a* have been omitted.

reversal potential was about -60 mV and -40 mV, respectively. These values should be compared with the value of -75 mV for the fast K^+ channels. After correction for leakage, the total outward current at 10 sec (Fig. 10*B*) is about 87·5 % of the peak value.

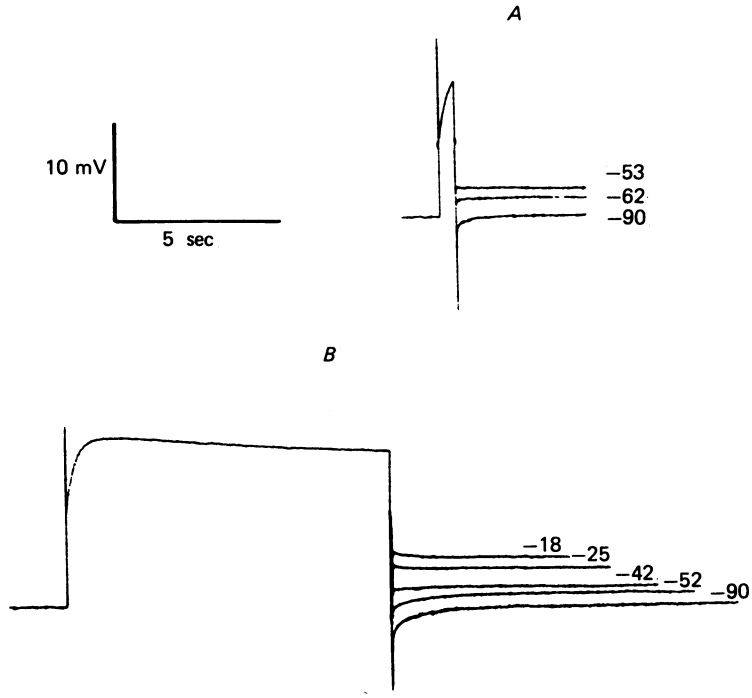

Fig. 10. ΔV records during long depolarizations in a slow fibre. Following a 0·5 sec (*A*) or 10 sec pulse (*B*) to $+5$ mV, the membrane potential was taken to the levels indicated in order to study slow tail currents. Records were taken with a chart recorder. Traces for -53 mV and -62 mV in *A* have been shifted upwards slightly. Control taken from V_2; holding potential $= -90$ mV. Same fibre as Fig. 3*B*; solution C; 5·6 °C.

There are several possible explanations for this small droop, for the slow tail currents, and for the shifts in reversal potential. Accumulation of K^+ ions in the tubule system or activation of a slow inward current, or both, could be important. Slow inward Ca^{2+} currents (Beaty & Stefani, 1976; Stanfield, 1977; Palade & Almers, 1978) and delayed tubular K^+ currents (Kirsch, Nicols & Nakajima, 1977) have been observed in twitch fibres. Such currents might also exist in slow fibres.

Stefani & Uchitel (1976) have presented indirect evidence for a voltage dependent Ca^{2+} permeability in slow fibres, and activation of such a system with a time constant of several seconds might result in the droop of outward current (Fig. 10*B*). If the Ca^{2+} channels closed very slowly on repolarization, they might contribute to tail currents and account for part of the observed shifts in reversal potential.

At present, ionic permeabilities of the slow fibre tubule system are not known, but if delayed K^+ channels are present in these membranes, K^+ ions might accumulate in the tubular lumen during a long depolarization. The measured V_{rev} would be a

weighted average of the surface and tubular values of V_K. The time course of slow tail currents might again be influenced by the slow closing of K^+ channels, but would most likely be determined by the diffusion of KCl out of the tubule system.

DISCUSSION

Measurements of membrane currents in frog slow fibres confirm some conclusions from earlier studies using less direct methods. As suggested by Burke & Ginsborg (1956), frog slow fibres do show a time- and voltage-dependent increase in K^+ permeability upon depolarization. Fast and slow components of delayed rectification are present in slow fibres. The fast component in slow fibres differs from that in twitch fibres in several respects.

Maximum G_K of the fast component in a slow fibre is at least an order of magnitude smaller than that in a twitch fibre. The steady-state G_K–V curve in a slow fibre rises much less steeply with voltage. The curve in Fig. 6, for example, increases e-fold in about 15 mV as compared to a value of 3 mV in a twitch fibre (Almers, 1976; see also Chandler, Rakowski & Schneider, 1976, Fig. 8). Whether the fast K^+ conductance in slow fibres inactivates during a long depolarization is presently uncertain.

We have never obtained unequivocal evidence of inward ionic currents of any sort in slow fibres, and an approximate limit on their detectability can be set. Occasionally, a small negative-going dip in the current base line was seen before I_K began to develop. Such apparent inward currents were never larger than 1–2 $\mu A/cm^2$ and persisted at very positive levels of membrane potential, sometimes even increasing in amplitude. While it is possible that small, fast inward Na^+ currents could at least partially underlie these observations, it is more likely that they are due to an artifact introduced by subtracting control from test pulses. Some fibres showed no dips at all, and when a few examples were analyzed more carefully, it was found that the early phase of a subtracted inward ΔV trace followed nearly the same time course as the control ΔV trace. We cannot rule out the possibility that normal slow fibres may have some Na channels present, but $\bar{G}_K$ must be $< \sim 0{\cdot}02$ mS/cm^2, as compared with 60 mS/cm^2 in twitch fibres (Adrian *et al.* 1970*a*).

Similarly, if any slow inward current developed during the 96 msec pulses in Fig. 5, it could have been no larger than 1 or 2 $\mu A/cm^2$. Unfortunately, we have no data on long pulses in TEA^+ Ringer solution. Based on indirect measurements, Stefani & Uchitel (1976) calculated a maintained maximum inward Ca^{2+} current density of about 0·2 $\mu A/cm^2$ at 0 mV, corresponding to a $\bar{G}_{Ca}$ of only 1·3 $\mu S/cm^2$. Such currents would probably be well below our limit of resolution.

This work was supported by a grant from the U.S. National Institutes of Health (PHS NS 07474) to Dr W. K. Chandler and by a NIH Postdoctoral Fellowship to C.S.H. We would like to thank Dr Chandler for continuous encouragement and helpful advice throughout the course of this work, Drs R. W. Tsien, S. M. Baylor, and M. W. Marshall for suggestions on the manuscript, and Mr H. Fein and staff for construction and maintenance of equipment.

REFERENCES

ADRIAN, R. H. (1964). The rubidium and potassium permeability of frog muscle membrane. *J. Physiol.* **175**, 134–159.

ADRIAN, R. H., CHANDLER, W. K. & HODGKIN, A. L. (1970*a*). Voltage-clamp experiments in striated muscle fibres. *J. Physiol.* **208**, 607–644.

ADRIAN, R. H., CHANDLER, W. K. & HODGKIN, A. L. (1970*b*). Slow changes in potassium permeability in skeletal muscle. *J. Physiol.* **208**, 645–668.

ADRIAN, R. H. & PEACHEY, L. D. (1965). The membrane capacity of frog twitch and slow muscle fibres. *J. Physiol.* **181**, 324–336.

ALMERS, W. (1976). Differential effects of tetracaine on delayed potassium channels and displacement currents in frog skeletal muscle. *J. Physiol.* **262**, 613–637.

BEATY, G. N. & STEFANI, E. (1976). Inward calcium current in twitch muscle fibres of the frog. *J. Physiol.* **260**, 27–28*P*.

BLINKS, J. R. (1965). Influence of osmotic strength on cross-section and volume of isolated single muscle fibres. *J. Physiol.* **177**, 42–57.

BURKE, W. & GINSBORG, B. L. (1956). The electrical properties of the slow muscle fibre membrane. *J. Physiol.* **132**, 586–598.

CHANDLER, W. K., GILLY, W. F. & HUI, C. S. (1978). Electrical properties of amphibian slow muscle fibres. In *Biophysical Aspects of Cardiac Muscle*, ed. MORAD, M., pp. 31–44. New York: Academic Press.

CHANDLER, W. K., RAKOWSKI, R. F. & SCHNEIDER, M. F. (1976). Effects of glycerol treatment and maintained depolarization on charge movement in skeletal muscle. *J. Physiol.* **254**, 285–316.

CONTI, F. & PALMIERI, G. (1968). Nerve fiber behavior in heavy water under voltage clamp. *Biophysik* **5**, 71–77.

COSTANTIN, L. L. (1968). The effect of calcium on contraction and conductance thresholds in frog skeletal muscle. *J. Physiol.* **195**, 119–132.

DULHUNTY, A. F. & FRANZINI-ARMSTRONG, C. (1975). The relative contributions of the folds and caveolae to the surface membrane of frog skeletal muscle fibres at different sarcomere lengths. *J. Physiol.* **250**, 513–539.

DULHUNTY, A. F. & FRANZINI-ARMSTRONG, C. (1977). The passive electrical properties of frog skeletal muscle fibres at different sarcomere lengths. *J. Physiol.* **266**, 687–711.

GARBY, L. & NORDQVIST, P. (1955). The effect of deuterium oxide (heavy water) on conduction velocity in isolated frog nerve. *Acta physiol. scand.* **34**, 162–168.

GILLY, W. F. & HUI, C. S. (1980*a*). Mechanical activation in slow and twitch skeletal muscle fibres of the frog. *J. Physiol.* **301**, 137–156.

GILLY, W. F. & HUI, C. S. (1980*b*). Voltage-dependent charge movement in frog slow muscle fibres. *J. Physiol.* **301**, 175–190.

GODT, R. E., ALLEN, D. G. & BLINKS, J. R. (1978). Effects of deuterium oxide (D_2O) on calcium transients and myofibrillar responses in frog skeletal muscle. *Biophys. J.* **21**, 17a.

HODGKIN, A. L. & NAKAJIMA, S. (1972). The effect of diameter on the electrical constants of frog skeletal muscle fibres. *J. Physiol.* **221**, 105–120.

HUI, C. S. & GILLY, W. F. (1977). Membrane electrical properties of frog slow muscle fibers. *Biophys. J.* **17**, 4a.

KIRSCH, G. E., NICHOLS, R. A. & NAKAJIMA, S. (1977). Delayed rectification in the transverse tubules. Origin of the later after-potential in frog skeletal muscle. *J. gen. Physiol.* **70**, 1–21.

KUFFLER, S. W. & VAUGHAN WILLIAMS, E. M. (1953). Small-nerve junctional potentials. The distribution of small motor nerves to frog skeletal muscle, and the membrane characteristics of the fibres they innervate. *J. Physiol.* **121**, 289–317.

LYNCH, C. (1978*a*). Kinetic and biochemical separation of delayed rectifier currents in frog striated muscle. *Biophys. J.* **21**, 55a.

LYNCH, C. (1978*b*). Kinetic and biochemical separation of potassium currents in frog striated muscle. Ph.D. thesis, University of Rochester, New York, U.S.A.

NAKAJIMA, S. & KURODA, T. (1976). Effects of deuterium oxide on mechanosensory receptor. *Proc. natn. Acad. Sci. U.S.A.* **73**, 4703–4705.

NASLEDOV, G. A., ZACHAR, J. & ZACHAROVA, D. (1966). The ionic requirements for the development of contracture in isolated slow muscle fibres of the frog. *Physiologia bohemoslov.* **15**, 293–306.

PALADE, P. T. & ALMERS, W. (1978). Slow Na and Ca currents across the membrane of frog skeletal muscle fibres. *Biophys. J.* **21**, 168a.

PEACHEY, L. D. (1965). The sarcoplasmic reticulum and transverse tubules of the frog's sartorius. *J. cell Biol.* **25**, 209–232.

SCHNEIDER, M. F. & CHANDLER, W. K. (1976). Effects of membrane potential on the capacitance of skeletal muscle fibres. *J. gen. Physiol.* **67**, 125–163.

STANFIELD, P. R. (1970). The effect of the tetraethylammonium on the delayed currents of frog skeletal muscle. *J. Physiol.* **209**, 209–229.

STANFIELD, P. R. (1977). A calcium dependent inward current in frog skeletal muscle fibres. *Pflügers Arch.* **368**, 267–270.

STEFANI, E. & STEINBACH, A. B. (1969). Resting potential and electrical properties of frog slow muscle fibres. Effect of different external solutions. *J. Physiol.* **203**, 383–401.

STEFANI, E. & UCHITEL, O. D. (1976). Potassium and calcium conductance in slow muscle fibres of the toad. *J. Physiol.* **255**, 435–448.

SVENSMARK, O. (1961). The effect of deuterium oxide on the mechanical properties of muscle. *Acta physiol. scand.* **53**, 75–84.

THOMSON, J. R. (1963). *Biological Effects of Deuterium.* Oxford: Pergamon Press.